Applications and Simulations of a Discontinuous Oral Absorption Pharmacokinetic Model

Jennifer Wright Witcher[1] and F. Douglas Boudinot[1,2]

Received April 12, 1996; accepted August 23, 1996

Purpose. To illustrate the application of a discontinuous oral absorption model to cimetidine and ranitidine plasma concentration versus time data to demonstrate the use of the model for drugs which display discontinuous oral absorption profiles, and to illustrate the effect of various model parameters on plasma drug concentration versus time profiles and bioavailability.

Methods. A discontinuous oral absorption model was used to fit ranitidine and cimetidine serum concentrations following oral and intravenous administration. The model was also used to simulate bioavailability and plasma concentrations versus time profiles for various parameter values.

Results. Serum concentrations following administration of ranitidine and cimetidine were well described by the model, and parameter estimates obtained were in agreement with literature values. Simulations demonstrate the effects of various absorption parameters and gastrointestinal tract transit parameters on bioavailability and plasma concentration profiles.

Conclusions. This discontinuous oral absorption pharmacokinetic model can be a useful tool in characterizing absorption phases, disposition, and bioavailability of drugs exhibiting two absorption peaks following oral administration.

KEY WORDS: discontinuous absorption; bioavailability; cimetidine; ranitidine.

INTRODUCTION

A number of drugs display two absorption peaks following oral administration, including ranitidine (1, 2), cimetidine (3, 4), piretanide (5), and furosemide (6). Second peaks following oral administration may be due to enterohepatic recycling, discontinuous intestinal absorption, and variable gastric emptying. Enterohepatic recycling is unlikely if the second peak is observed after oral administration but not after intravenous administration. Evidence suggests that some drugs, such as ranitidine and cimetidine, are absorbed from two separate sites (2, 8, 9) resulting in discontinuous absorption. Variability in gastric emptying rate may account for varying amounts of drug available for absorption in the small intestine over time (4) resulting in two absorption peaks. Both of these situations can be described as multiple phases of absorption.

The physiological reason for a second absorption peak is often not delineated until further mechanistic investigations are performed. However, pharmacokinetic parameters must still be obtained from plasma concentration-time data which exhibit the two absorption peaks. Recently, a discontinuous oral absorption pharmacokinetic model was developed to describe plasma concentrations of 1-(2-fluoro-5-methyl-β-L-arabinofuranosyl)-uracil (L-FMAU), a nucleoside analogue which displayed two absorption peaks following oral administration (10). The discontinuous oral absorption site model characterized the data well, and pharmacokinetic parameter estimates were in agreement with those obtained by non-compartmental analysis (11). Further, bioavailability determined using the model was in agreement with standard area under the curve and urinary excretion methods.

Previously, pharmacokinetic models have been developed to analyze this type of oral absorption data (12–14). However, this method is unique in that differential equations can be written to describe the model and used directly to fit the plasma concentrations using intravenous and oral data simultaneously. Oral absorption parameters can be generated and bioavailability can also be calculated using this model. Further, no assumptions concerning the physiological location of absorption sites in the GI tract must be made to utilize the model. Overall, this is a relatively simple and direct method of data analysis for this type of oral absorption phenomenon.

The objective of the present work was to illustrate the application of the discontinuous oral absorption model to cimetidine and ranitidine. In addition, simulations were performed to demonstrate the effect of model parameters on plasma concentration versus time profiles and bioavailability.

METHODS

The discontinuous oral absorption model (Figure 1) was developed as previously described (10). In this pharmacokinetic model, the oral dose of drug, $Dose_{PO}$, is given into the GI_{A1} compartment, which is the first absorption site. Absorption from the first site is described by first-order rate constant k_{a1}. Drug which remains in the gastrointestinal tract travels to the transit GI compartment, GI_T, a non-absorbing region of the GI tract. Transit to this compartment is described by first-order GI transit rate constant k_{t1}. Essentially, this transit rate constant describes the rate at which drug leaves the first absorption site. Drug then travels to the second absorbing region, GI_{A2}, by first-order GI transit rate constant k_{t2}. Absorption from the second

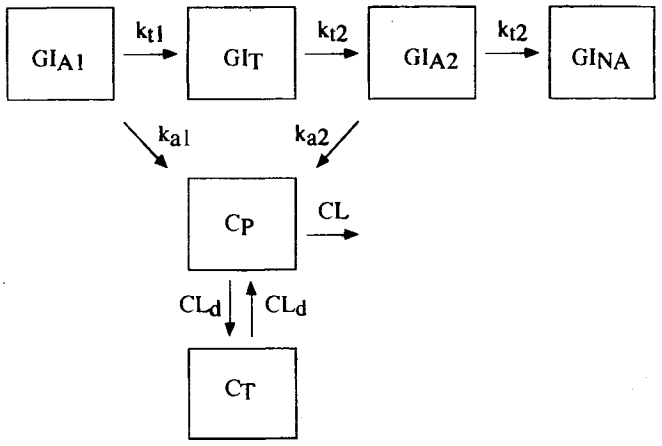

Fig. 1. Discontinuous oral absorption pharmacokinetic model.

[1] Department of Pharmaceutics, College of Pharmacy, University of Georgia, Athens, Georgia 30602.
[2] To whom correspondence should be addressed.

0724-8741/96/1100-1720$09.50/0

absorbing region is described by first-order rate constant k_{a2}. All drug remaining in the *GI* tract subsequently travels to the GI_{NA} compartment, which represents the amount of drug which is not absorbed in either absorption phase.

Drug absorption to the central compartment occurs as a result of two absorption phases or regions, k_{a1} and k_{a2}, and results in plasma concentrations, C_P. The volume of the central compartment is described by V_C. Drug is distributed to the peripheral compartment by distributional clearance, CL_d, resulting in a tissue concentration, C_T, in a tissue volume, V_T. Elimination of drug from the central compartment is represented by systemic clearance, *CL*.

The differential equations for this model are given as Equations 1–8. These equations were fit to plasma concentrations following intravenous (Equations 1 and 2) and oral (Equations 3–8) administration by nonlinear least-squares regression analysis using the Gauss-Newton algorithm in PCNONLIN with a weighting factor of $1/C_P$.

$$\frac{dC_P}{dt} = -\frac{CL}{V_C}C_P - \frac{CL_d}{V_C}C_P + \frac{CL_d}{V_C}C_T \quad (1)$$

$$\frac{dC_T}{dt} = \frac{CL_d}{V_T}C_P - \frac{CL_d}{V_T}C_T \quad (2)$$

$$\frac{dC_P}{dt} = \frac{k_{a1}}{V_C}GI_{A1} + \text{TSTAR}\frac{k_{a2}}{V_C}GI_{A2} - \frac{CL}{V_C}C_P - \frac{CL_d}{V_C}C_P + \frac{CL_d}{V_C}C_T \quad (3)$$

$$\frac{dC_T}{dt} = \frac{CL_d}{V_T}C_P - \frac{CL_d}{V_T}C_T \quad (4)$$

$$\frac{dGI_{A1}}{dt} = -k_{t1}GI_{A1} - k_{a1}GI_{A1} \quad (5)$$

$$\frac{dGI_T}{dt} = k_{t1}GI_{A1} - k_{t2}GI_T \quad (6)$$

$$\frac{dGI_{A2}}{dt} = k_{t2}GI_T - k_{t2}GI_{A2} - \text{TSTAR}k_{a2}GI_{A2} \quad (7)$$

$$\frac{dGI_{NA}}{dt} = k_{t2}GI_{A2} \quad (8)$$

A binary switch function, TSTAR, in the equations describes the initiation of absorption from the GI_{A2} compartment. The switch function constant *B*, which was the time absorption from GI_{A2} began, was used in the PCNONLIN subroutine. Before time *B*, the TSTAR value was zero, and after time *B*, TSTAR was 1.

Ranitidine and Cimetidine

Plasma concentration versus time data for ranitidine (1) and cimetidine (15) were obtained from the literature. Equations 1–8 were fit simultaneously to plasma concentrations following oral and intravenous administration of ranitidine and cimetidine.

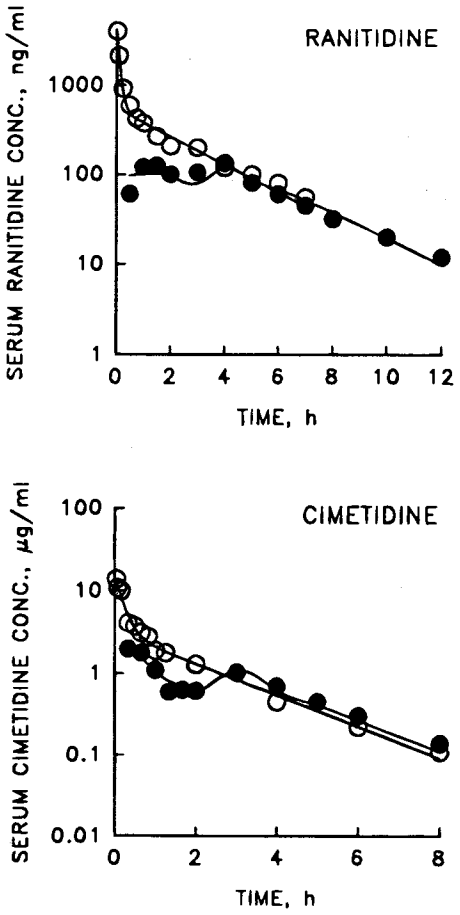

Fig. 2. Serum ranitidine and cimetidine concentrations versus time following intravenous (○) and oral (●) administration. Symbols represent observed data and lines represent fitted curves.

Initial estimates for *CL*, CL_d, V_C, and V_T were obtained from analysis of intravenous data alone, and an initial estimate for *B* was obtained by visual inspection of the concentration-time profiles. Through an iterative process of holding some parameters constant, estimates were obtained for *B*, k_{a1}, k_{a2}, k_{t1}, k_{t2}, *CL*, CL_d, V_C, and V_T. If varying the estimates for parameters did not change the values generated by PCNONLIN, a global minimum was assumed.

Simulations

The discontinuous oral absorption model was used to simulate plasma concentration versus time data for various absorption rate constant, *GI* transit rate constant, and *B* values. Values for V_C, V_T, *CL*, and CL_d used as constants in the simulations were obtained from analysis of the ranitidine data. Simulations were performed in which one parameter was varied while all other parameters were held constant. Values for k_{a1} were varied from 0.1 to 4.0 h^{-1}, k_{a2} from 0.1 to 1.6 h^{-1}, k_{t1} from 0.1 to 2.0 h^{-1}, k_{t2} from 0.05 to 2.0 h^{-1}, and *B* was varied from 0.5 to 3.5 h. When employed as constants, *B* was 2.5 h, k_{a1} and k_{a2} were 0.4 h^{-1}, and k_{t1} and k_{t2} were 1.0 h^{-1}. The cumulative amount of drug in the GI_{NA} compartment (GI^{∞}_{NA}) was considered

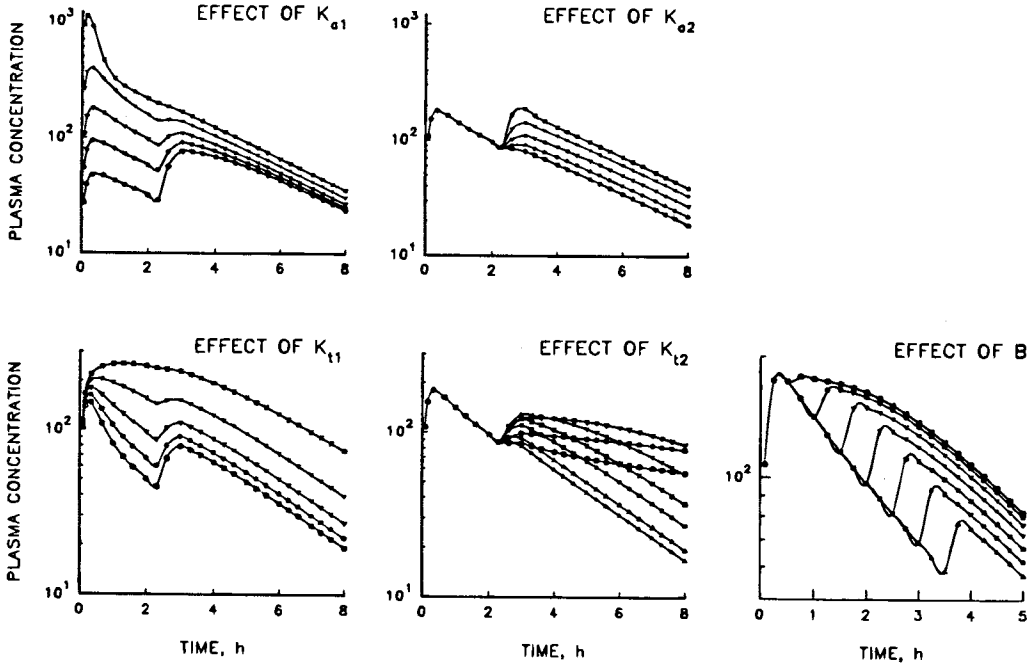

Fig. 3. *Effect of* k_{a1}: Simulations of plasma concentrations versus time showing the effect of varying k_{a1} from 0.1 to 4 h^{-1} while holding other parameters constant. *Effect of* k_{a2}: Simulations of plasma concentrations versus time showing the effect of varying k_{a2} from 0.1 to 1.6 h^{-1} while holding other parameters constant. *Effect of* k_{t1}: Simulations of plasma concentrations versus time showing the effect of varying k_{t1} from 0.1 to 2 h^{-1} while holding other parameters constant. *Effect of* k_t^2: Simulations of plasma concentrations versus time showing the effect of varying k_{t2} from 0.05 to 2 h^{-1} while holding other parameters constant. *Effect of B*: Simulations of plasma concentrations versus time showing the effect of varying B from 0.5 to 3.5 h while holding other parameters constant.

to be the amount of drug not absorbed and was used to calculate bioavailability (F) as shown in Equation 9.

$$F = \frac{\text{Dose}_{PO} - GI^{\infty}_{NA}}{\text{Dose}_{PO}} \quad (9)$$

RESULTS AND DISCUSSION

Ranitidine serum concentrations (Figure 2) were well described by the discontinuous oral absorption model. Following intravenous administration, ranitidine serum levels declined rapidly in a biexponential manner. After oral administration, two absorption peaks were observed with the second peak occurring approximately 4 h after dose administration. Equations 1–8 were fit to the intravenous and oral data and pharmacokinetic parameter estimates were obtained. Total clearance was 51.6 ± 9.2 *L*/h (mean ± standard error), and distributional clearance was 134.7 ± 26.2 *L*/h. Volume of the central compartment was 21.4 ± 3.9 *L*, and volume of the tissue compartment was 90.8 ± 18.3 *L*. These parameter estimates were in agreement with the literature values for total clearance of 45.6 *L*/h and V_{area} of 132.9 *L* (1). Bioavailability determined from the oral absorption model was 61%, which is in close agreement with the literature value of 52 ± 11% (mean ± SD). Estimates for B, k_{a1}, k_{a2}, k_{t1}, and k_{t2} were 3.7 h, 0.18 h^{-1}, 5.16 h^{-1}, 0.47 h^{-1}, and 1.85 h^{-1}, respectively.

Cimetidine serum concentrations (Figure 2) were also well described by the discontinuous oral absorption model. Using Equations 1–8, total clearance was estimated as 30.6 ± 2.5 *L*/h, and distributional clearance was 46.3 ± 6.4 *L*/h. Volume of the central compartment was 18.5 ± 1.6 L, and volume of the tissue compartment was 34.0 ± 4.7 L. These parameter estimates are in agreement with the literature values of total clearance of 33.5 *L*/h and steady-state volume of distribution of 65.5 *L* (15). Bioavailability calculated using the model was 56%, which is in close agreement with the literature value of 54%. Estimates for B, k_{a1}, k_{a2}, k_{t1}, and k_{t2} were 2.4 h, 1.3 h^{-1}, 5.0 h^{-1}, 2.3 h^{-1}, and 1.0 h^{-1}, respectively.

Absorption parameter estimates for both ranitidine and cimetidine suggest there is a second absorption site with an absorption rate constant greater than that of the first site. It is interesting that both ranitidine and cimetidine had k_{a2} values of approximately 5 h^{-1}, which were greater than the k_{a1} values for both drugs. If the drugs were absorbed from a single site in the *GI* tract in 2 absorption phases resulting from variable gastric emptying, the k_{a1} and k_{a2} values should be approximately equal. However, k_{a1} and k_{a2} values were different for both drugs supporting the two absorption site theory.

Simulations performed using the discontinuous oral absorption model to illustrate the effect of the absorption rate constants, k_{a1} and k_{a2}, on plasma concentration versus time curves are shown in Figure 3. The magnitude of k_{a1} had a great influence on the plasma concentration versus time profiles and bioavailability. The magnitude of k_{a2} also influenced the AUC, but not as much as k_{a1}. There was a direct relationship between the magnitude of the absorption rate constants and the shape of the plasma concentration versus time curve. As the magnitude

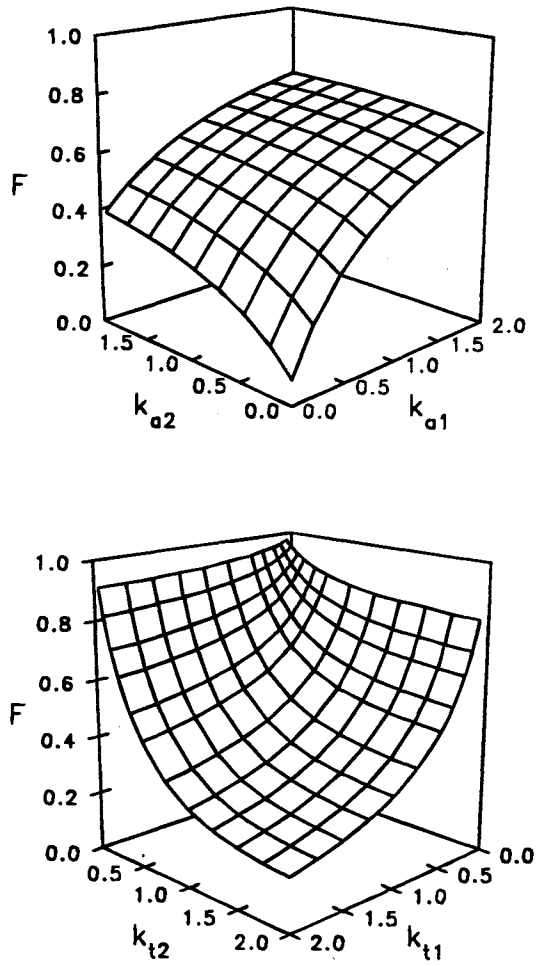

Fig. 4. Three dimensional plots illustrating the effect of k_{a1} and k_{a2}, and k_{t1} and k_{t2}, respectively, on bioavailability calculated from simulations using the discontinuous oral absorption model.

of the absorption rate constants increased, higher plasma concentrations were achieved and sharper increases in the plasma concentrations were observed.

Figure 4 illustrates the effect of k_{a1} and k_{a2} on bioavailability. As k_{a1} and k_{a2} values approached zero, bioavailability also approached zero. As the absorption rate constant values increased, bioavailability increased. The first absorption site (k_{a1}) appeared to have a greater effect on bioavailability than did k_{a2}. At higher k_{a1} values, absorption from the first absorption site was essentially complete, and thus the contribution of the second absorption site to bioavailability was negligible. Above k_{a1} and k_{a2} values of 1.0 h^{-1}, the increase in bioavailability reached a plateau, and further increases in k_{a1} and k_{a2} values did not have a great influence on bioavailability.

Simulations were also performed to examine the effect of *GI* transit rate constants, k_{t1} and k_{t2}, on plasma concentration versus time curves (Figure 3). The magnitude of k_{t1} represents the rate at which drug is leaving the first absorption site. An inverse relationship between k_{t1} and the plasma concentrations achieved was observed. The faster the drug leaves the first absorption site, the lower the resulting plasma concentrations. An interesting aspect about this figure is the shape of the plasma concentration profile at the lowest value of k_{t1} (0.1 h^{-1}). As the value of k_{t1} approaches zero, the rate the drug leaves the first absorption site decreased. Thus, absorption continues to occur from the first site, and the two absorption phases are no longer distinct.

Simulations showing the effect of k_{t2} are shown in Figure 3. The magnitude of k_{t2} indicates the rate at which drug is reaching and departing the second absorption site. The k_{t2} value of 0.25 h^{-1} resulted in the greatest plasma concentrations. For k_{t2} values above 0.25 h^{-1}, there was an inverse relationship between the k_{t2} value and plasma concentrations. As k_{t2} increased, drug leaves the second absorption site at a faster rate, therefore the resulting plasma concentrations are lower. As k_{t2} approaches zero, a sustained absorption phenomenon occurs and the plasma concentration versus time curve levels off. Essentially, the drug is stationary in the second absorption site and continues to undergo absorption.

Figure 4 shows the effect of k_{t1} and k_{t2} on bioavailability. The *GI* transit rate constants appeared to greatly influence the bioavailability. A significant increase in bioavailability was observed as k_{t1} and k_{t2} approach zero. As k_{t1} and k_{t2} approached zero, the rate at which the drug leaves the absorption site also approached zero. Therefore, the extent of absorption was greater. As k_{t1} and k_{t2} increased above 1 h^{-1}, the decrease in bioavailability reached a plateau and was not as greatly affected by the *GI* transit rate constant.

Simulations were also performed to examine the effect of *B* (Figure 3), the time at which the second absorption phase is initiated, on plasma concentration versus time profiles and bioavailability. Although the *B* value greatly influenced shape of the plasma concentration versus time curve, bioavailability was not as greatly affected. As *B* increased from 0.5 to 3.5 h, bioavailability decreased from 0.49 to 0.34. At the *B* value of 0.5 h, the plasma concentration versus time profile closely resembles the profile of a single absorption site.

CONCLUSIONS

The disposition of drugs exhibiting two absorption peaks following oral administration is often difficult to characterize. The discontinuous oral absorption pharmacokinetic model developed in this report can be a useful tool for characterizing absorption phases and generating pharmacokinetic parameters for these drugs.

ACKNOWLEDGMENTS

Jennifer Wright Witcher was supported by a SmithKline Beecham-AFPE Pharmaceutics/Biopharmaceutics Fellowship.

REFERENCES

1. D. C. Garg, D. J. Weidler, and F. N. Eshelman. *Clin. Pharmacol. Ther.* **33**:445–452 (1983).
2. M. F. Williams, G. E. Dukes, W. Heizer, Y.-H. Han, D. J. Hermann, T. Lampkin, and L. J. Hak. *Pharm. Res.* **9**:1190–1194 (1992).
3. S. S. Walkenstein, J. W. Dubb, W. C. Randolph, W. J. Westlake, R. M. Stote, and A. P. Intoccia. *Gastroenterology* **74**:360–364 (1978).
4. R. L. Oberle and G. L. Amidon. *J. Pharmacokin. Biopharm.* **15**:529–545 (1987).
5. D. Brockmeier, H.-G. Grigoleit, and H. Leonhardt. *Eur. J. Clin. Pharmacol.* **30**:79–82 (1986).
6. M. M. Hammarlund, L. K. Paalzow, and B. Odlind. *Eur. J. Clin. Pharmacol.* **26**:197–207 (1984).
7. R. Gugler, A. Somogy, and Kv. Bergman. *Clin. Pharmacol. Ther.* **29**:249–250 (1981).

8. T. Gramatté, E. El Desoky, and U. Klotz. *Eur. J. Clin. Pharmacol.* **46**:253–259 (1994).
9. T. Funaki, S. Furuta, and N. Kaneniwa. *Int. J. Pharm.* **31**:119–123 (1986).
10. J. D. Wright, T. Ma, C. K. Chu, and F. D. Boudinot. *Biopharm. Drug Dispos.* **17**:197–207 (1996).
11. J. D. Wright, T. Ma, C. K. Chu, and F. D. Boudinot. *Pharm. Res.* **12**:1350–1353 (1995).
12. A. B. Suttle, G. M. Pollack, and K. L. R. Brouwer. *Pharm. Res.* **9**:350–356 (1992).
13. T. Funaki, N. Watari, S. Furuta, and N. Kaneniwa. *Int. J. Pharm.* **43**:59–65 (1988).
14. K. Murata, K. Noda, K. Kohno, and M. Samejima. *J. Pharm. Sci.* **76**:109–113 (1987).
15. D. R. P. Guay, G. R. Matzke, H. N. Bockbrader, and J. Dancik. *Clin. Pharm.* **2**:157–162 (1983).